21

Multi-Aspect Comparative Detection of Lesions in Medical Images

Juliusz Kulikowski and Malgorzata Przytulska
M. Nalecz Institute of Biocybernetics and Biomedical Engineering, PAS Warsaw, Poland

1. Introduction

Symmetry is an easily observable property of a normal human body. It also occurs in the anatomy of some of its organs: motion or sensory organs, brain, dentition, breasts, kidneys, etc. This property is often used as a basis of visual diagnosis of anatomical defects or of pathological lesions in the organs, expressed by local disparities between the (generally symmetric) pairs of compared images (Rogowska J., Preston K., Hunter G.J. & al., 1995). Such approach, based on an assumption that in most cases the defects or lesions have been caused by asymmetrically acting factors, leads to a simple algorithm of lesions detection by pixel-from-pixel subtraction of matched pairs of images. However, for several reasons this approach does not lead to satisfactory results: 1st a general symmetry of normal body organs does not mean that small anatomic differences in them cannot occur, 2nd small local differences in compared pixel values can also be caused by image acquisition defects, 3rd substantial differences may be hidden in specific subtle local morphological structure of analyzed organs. A comparative detection of lesions is thus a non-trivial problem needing advanced solution approach. This remark also concerns a comparison of acquired at distanced time-instants medical images of a given organ aimed at an assessment of the results of its medical treatment. A comparative lesions detection should consist not so much in a detection of any formal but rather of *medically significant* differences between the compared images. Medically significant image details may be manifested by occurrence of both simple differences between the local (monochromatic or multi-chromatic) pixel values as well as by occurrence of more subtle features characterizing local sub-areas in the examined images. This leads to a concept of comparative image analysis based on a *multi-aspect dissimilarity measure* (Kulikowski J. L., Przytulska M., 2009a). The notions of *similarity* and *dissimilarity* are evidently related: the more similar two objects are, the less they are dissimilar. In certain cases, when the objects can be considered as elements of a metric (e.g. Euclidean) space their dissimilarity can strongly be connected with a *distance* between them. However, not all objects of medical interest, usually described by combinations of their quantitative and qualitative features, as the elements of a formally defined metric space can be considered. That is why it seems more reasonable to define dissimilarity (as well as similarity) measure as a normalized dimensionless parameter. Using the notion of *multi-aspect dissimilarity* to comparative lesions detection seems not only to be intuitively justified but also more suitable to distinguish between the normal and pathological tissues than a distance notion.

The aim of this Chapter is presentation of an approach to computer-aided comparative analysis of medical images aimed at detection of lesions occurring in one of two symmetrically located body regions. In this approach the concept of *multi-aspect similarity measure* as well as of a based on it concept of *dissimilarity measure* presented in the mentioned paper (Kulikowski J. L., Przytulska M., 2009a) plays a basic role. Moreover, application of *morphological spectra*, originally presented in some former papers (Kulikowski J. L., Przytulska M., 2007a; Kulikowski J. L., Przytulska M, & Wierzbicka D., 2007b), is also presented in a context of multi-aspect similarity of biological tissues assessment. It will be shown how the above-mentioned concepts can be used to an iterative lesions detection process consisting in a step-wise reinforcing of the objects' discrimination criteria. The below-presented methods have been primarily tested on cerebral single photon emission tomography (*SPECT*) as well as on liver ultrasound elastography (*USE)* images and some results of those experiments will be shown below.

2. Formal model of lesions

A *lesion* can be defined as a *harmful change in the tissues of bodily organs, caused by injury or disease* (Hornby A.S., 1980). In computer-aided medical images analysis we are interested not only in a simple lesions detection but also in their localization (e.g. by contouring), size and form description, intensity assessment, etc. Of course, it is assumed that any lesion area is visually from the background distinguishable. However, 1st not all visual differences are for lesion detection substantial, and 2nd it may a priori be not known how a certain sort of lesion should visually be manifested. Lesion detection reminds thus detection of a pickpocket in a crowd of bus passengers: we know, that his behavior differs from this of other passengers, however, the face and wear differences for his reliable detection are not sufficient.

A comparative lesions detection is thus based on the following assumptions:

a. there is given a finite sequence of pairs of related images presenting symmetrically located organs or parts of a bodily organ available in different projections;
b. the lesion of interest in no more but one (and always the same) image of any pair is expected;
c. two types of local differences between the images of any pair are possible:
    1. substantial differences caused by occurring a lesion in one and lack in other one side of the examined organ;
    2. irrelevant differences caused by objects different positioning, secondary anatomical details existence, inaccurate pairs of images symmetry fixation, image distortions etc.;
d. the form, size and even the occurrence of lesion in different pairs of images within a given sequence may be different.

In Fig. 1 several examples of pairs of medical images prepared for comparative analysis are shown. In the images the pairs of symmetrical *regions of interest* (*ROI*s) on which the analysis is to be focused are marked by black rectangular contours. Note that not all differences for comparative analysis have been chosen there; their primary selection is usually done by an experienced medical specialist, the role of computer system is secondary, consisting in aiding the analysis: making its results more accurate and comparable if repeated several times.

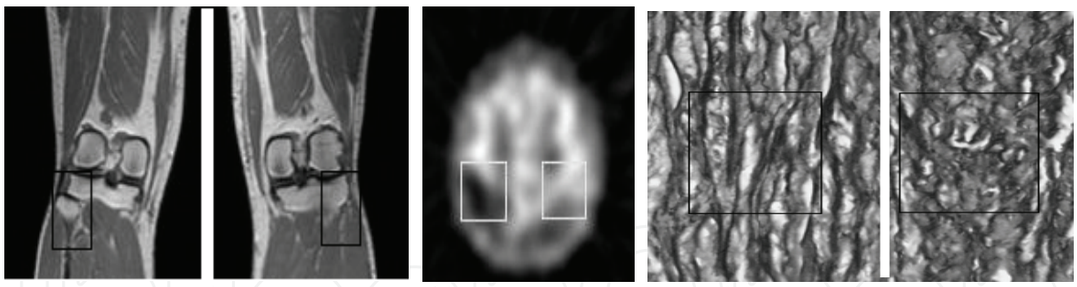

a) b) c)

Fig. 1. Pairs of medical images prepared for comparative analysis: a) radiological images of knees, b) *SPECT* image of brain, c) microscopic image of aorta tissue.

For comparative image analysis two basic types of image features can be used:

1. Primary, local features obtained by a direct point-to-point comparison of images:
   a. pixels' intensity levels,
   b. pixels' color components.
2. Secondary, environmental features defined and calculated as functions of pixel values in selected image fragments:
   a. spectral characteristics,
   b. statistical characteristics,
   c. fractal characteristics,
   d. micro-morphological characteristics,

etc. Local features neglect any spatial relationships between pixel values in the examined images. It can be observed in Fig. 2 where a *SPECT* image of a brain a) and its mirror-inversion b) have been subtracted in order to visualize the difference of respective pixel intensities c). The spots in Fig. 2.c) correspond to the regions of high brightness disparities in the compared brain hemispheres. However, no subtle differences of textures using this type of visualization can be detected.

Environmental features take into account spatial relationships within some regular (e.g. square or rectangular) sub-areas, called *basic windows*, covering the *ROI*s. The form of *ROI* is not obviously rectangular, as shown in Fig. 3. However, identical form and size of a pair of *ROI*s make their analysis easier. Black points in Fig. 3 represent image elements (pixels), adjacent basic windows of 4×4 pixels size are separated by dotted lines, the area under

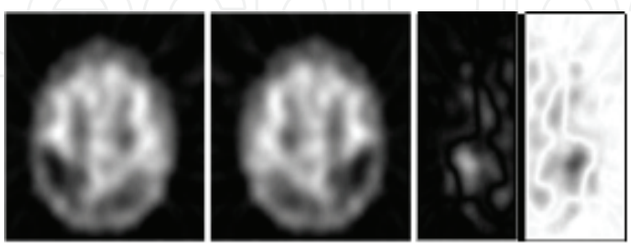

a) b) c)

Fig. 2. Result of subtraction of a *SPECT* brain image a) and its mirror-reflection b) visualizing the difference of respective pixel intensities c).

examination (*ROI*) consisting of a compact subset of basic windows has been contoured by a continuous line.

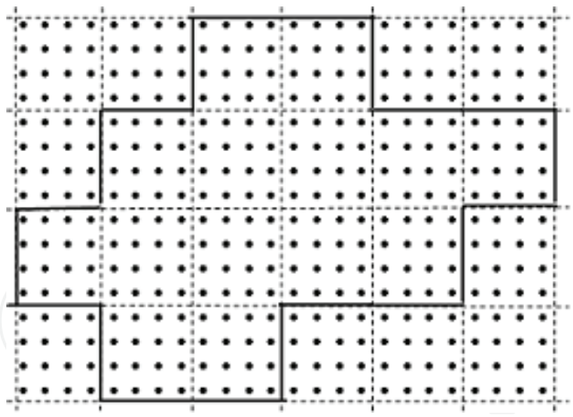

Fig. 3. Example of a region of interest (*ROI*) composed of basic windows.

An exact delineation of symmetrical pairs of *ROI*s needs taking both anatomical details and measurable geometrical image parameters into consideration. Before starting a computer-aided comparative lesions detection the images, if necessary, to a preliminary, symmetry correcting procedure should be subjected (Lester H., Arrige S.R., 1999). However, even in this case some remaining deficiencies of symmetry may affect the detection quality and this in design of lesions detection procedures should be taken into consideration.

Let us take into consideration a pair *A′, A″* of *ROI*s selected for comparative analysis. There will be denoted by *M* the number of basic windows in a *ROI* and by *N* be the number of pixels in a basic window. In most medical imaging modalities, like *X*-ray, ultrasound (*USG*), computer tomography (*CT*), single photon emission computer tomography (*SPECT*), positron emission tomography (*PET*), nuclear magnetic resonance (*NMR*), monochromatic images are dealt with; otherwise, pixel values should be represented by triplets of numbers corresponding to basic, e.g. *RGB*, *HSV*, *CMY*, *YIQ* etc. color components (Foley J.D., Van Dan A., Feiner S.K. & al., 1994). Below, monochromatic images are considered; however, the methods presented on more general cases can easily be extended.

For comparative image analysis based on local features the contents of a pair of *ROI*s of identical form and size can be represented by two $M \times N$ matrices:

$$\boldsymbol{U}' = [u'_{\mu\nu}],\ \boldsymbol{U}'' = [u''_{\mu\nu}],\ \mu \in [1,\ldots,M],\ \nu \in [1,\ldots,N], \tag{1}$$

where $u'_{\mu\nu}$, $u''_{\mu\nu}$ are pixel values belonging to a finite discrete space (brightness scale):

$$X = [0,1,\ldots,K-1] \tag{2}$$

value 0 being assigned to the maximum darkness. We also shall denote by

$$\boldsymbol{u}'_{\mu^*} = [u'_{\mu 1}, u'_{\mu 2},\ldots, u'_{\mu N}],\ \boldsymbol{u}''_{\mu^*} = [u''_{\mu 1}, u''_{\mu 2},\ldots, u''_{\mu N}],\quad \mu \in [1,\ldots,M], \tag{3}$$

the respective rows assigned to the basic windows, identically enumerated in both *ROI*s, and by

$$(\boldsymbol{u}'_{*\nu})^{tr} = [u'_{1\nu}, u'_{2\nu},\ldots, u'_{M\nu}],\ (\boldsymbol{u}''_{*\nu})^{tr} = [u''_{1\nu}, u''_{2\nu},\ldots, u''_{M\nu}],\ \nu \in [1,\ldots,N], \tag{4}$$

the (in transposed form presented here) columns of $\boldsymbol{U}'$ and $\boldsymbol{U}''$. Evidently, $\boldsymbol{u}'_{\mu^*}$ and $\boldsymbol{u}''_{\mu^*}$ represent the basic windows' contents while $\boldsymbol{u}'_{*\nu}$ and $\boldsymbol{u}''_{*\nu}$ collect the related components from the basic windows in the given *ROI*s.

We consider the vectors $\boldsymbol{u}'_{\mu^*}$, $\boldsymbol{u}''_{\mu^*}$ as elements of a N-dimensional discrete vector space X^N. The M-row matrices $\boldsymbol{U}'$ and $\boldsymbol{U}''$ represent thus two M-element subsets in X^N. The subsets can geometrically be presented as sets of points surrounded by "clouds" (*similarity areas* denoted, respectively, by Ξ' and Ξ'') of other points (vectors) similar to those of U' and U'', as illustrated by Fig. 4.

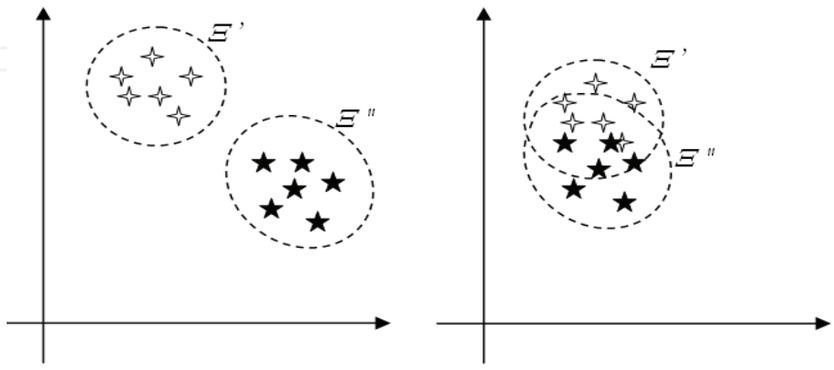

a) b)

Fig. 4. Geometrical illustration of the contents of two *ROI*s and their similarity areas Ξ', Ξ'': a) easily separable (dissimilar) subsets of vectors, b) similar subsets of vectors.

For comparative lesions detection not so much vectors representing basic windows but rather their differences $\boldsymbol{\xi}_{\mu^*} = \boldsymbol{u}'_{\mu^*} - \boldsymbol{u}''_{\mu^*}$ are of particular interest. A condensation of difference vectors close to the initial point of coordinates, as it is shown in Fig. 5 below, corresponds to high similarity of basic windows contents.

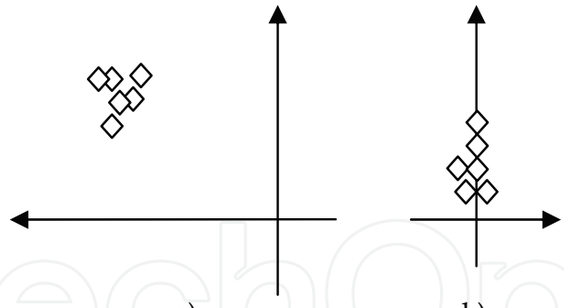

a) b)

Fig. 5. Differences of pairs of vectors corresponding to the sets Ξ' and Ξ''.

The notion of similarity area below will be more exactly defined. However, it follows from the above-made assumption c)-ii that even if significant disparities between the similarity areas Ξ' and Ξ'' (like those in Fig. 5 a) exist, they may be caused both by relevant as well as *i*rrelevant factors. Some of them (e.g. those caused by small anatomical details) by a compensation technique can be removed. Removing other irrelevant differences needs more sophisticated methods using as it later on will be shown. Finally, at each step of an iterative lesions detection process it is assumed that the dissimilarities between objects within similarity areas Ξ' and Ξ'' are mostly irrelevant while those between Ξ' and Ξ'' are mostly relevant to the diagnostic purposes. The comparative lesions detection problem can thus roughly be formulated as follows:

Assume that Ξ' and Ξ'' are two subsets in X^N containing vectors in a certain sense *similar*, respectively, to those of U' and U''; check belonging of a significant part of vectors of U' and U'' to the intersection $\Xi' \cap \Xi''$.

Positive checking results mean that no significant differences between the vectors of $\boldsymbol{U'}$ and $\boldsymbol{U''}$ have been detected; hence, A' and A'' are covered by non-distinguishable types of texture. Taking into account the above formulated assumption b) of comparative image analysis this leads to a conclusion that no lesion in the given pair of *ROI*s has been detected. Otherwise, a detected *dissimilarity* between $\boldsymbol{U'}$ and $\boldsymbol{U''}$ suggests that a lesion in one of *ROI*s can be suspected. Is it a real lesion, depends on the relevance of the differences to medical expectations, as it has been mentioned. However, in the above formulated problem some notions should be explained; what do they: *similar*, *similarity area, significant part* or *dissimilarity*, exactly mean? This will be explained below.

3. Similarity and dissimilarity measures

The terms: *similar* and *dissimilar* as commonly used seem to be intuitively clear. In a formal sense they correspond to a relation between some objects satisfying the following conditions:

1. Each object is similar to itself (*reciprocity of similarity*);
2. If object ω′ is similar to ω″ then ω″ is similar to ω′ (*symmetry of similarity*).

Similarity is thus a sort of *neighborhood relation*. In *dissimilarity* relation symmetry holds as well; however, this relation is not reciprocal. In both cases a question of their *transitivity* arises: if an object ω′ is similar to ω″ and ω″ is similar to ω‴, does it mean that ω′ is similar to ω‴? Undoubtedly, it is so in the case of similarity of triangles (among all possible triangles on an Euclidean plain) or similarity of all animals included into a given biological species. On the other hand, it may be not true if visual similarity of some objects is considered. E.g., if A (a son) is similar to B – his father (and vice versa, B is similar to A) as well as C (a sister of A) is similar to A, then not obviously C is similar to B (for example, because A and C were born by the same mother but have different fathers). The problem of a limited transitivity of similarity is illustrated in Fig. 6; the closer are any two patterns the higher is their similarity, external patterns a) and h) being totally dissimilar.

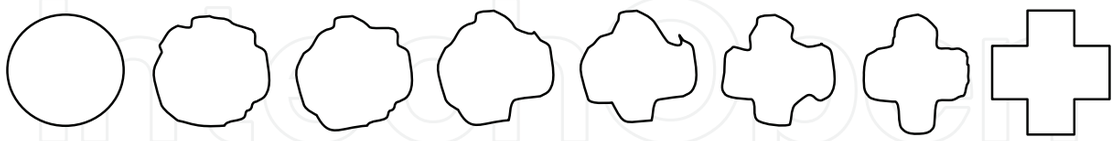

Fig. 6. A sequence of geometrical patterns whose similarity depends decreasingly on their distance in the row.

Evidently, it is reasonable to distinguish a *strong similarity* satisfying the transitivity condition and a *weak similarity* where transitivity is not satisfied or is satisfied within some limits only. Non-transitivity of similarity may also be caused by the fact that similarity of objects can be assessed in practice from different points of view when different pairs of objects are taken into consideration. This is illustrated in Fig. 7. The position, color and form of triangles have been taken into consideration as different aspects of similarity of triangular patterns.

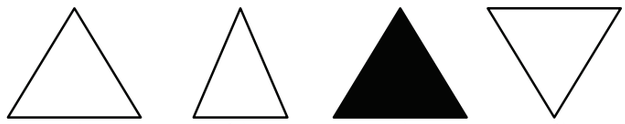

Fig. 7. Different aspects of similarity of triangular patterns: 1^0 a), b) and c) – from their position point of view, 2^0 a), b) and d) – from their color point of view, 3^0 a), c) and d) – from their form point of view.

Therefore, it arises a problem of a general, multi-aspect objects' similarity definition. This will be done below by definition of a *similarity measure*. Many proposals of definition of this notion can be found in literature (Gotlieb C. C., Kumar S., 1968; Bonner R. E., 1954). However, not all of them are flexible enough to take into account the multi-aspect nature of similarity into consideration. The below-given definition, as it has been shown in (Kulikowski J. L., 2001) makes it possible.

Definition 1.

Let Ω denote any set consisting of more than 2 elements (objects). We call *similarity measure* a function σ described on a Cartesian product Ω^2 satisfying the conditions:

$$\left.\begin{aligned} &\text{a/ } 0 \le \sigma(\omega',\omega'') \pounds 1, \\ &\text{b/ } \sigma(\omega',\omega') = 1, \\ &\text{c/ } \sigma(\omega',\omega'') = \sigma(\omega'',\omega') \\ &\text{d/ } \sigma(\omega',\omega'') \cdot \sigma(\omega'',\omega''') \le \sigma(\omega',\omega''') \end{aligned}\right\} \tag{5}$$

for any $\omega',\omega''\ \omega''' \in \Omega$.

Condition b/ corresponds to a reciprocity while c/ to a symmetry of similarity; a/ and b/ show also that 0 is the minimal and 1 is the maximal similarity measure of any two objects. Condition d/ reminds a so called *triangle inequality* in a distance measure definition (Rasiowa H., Sikorski R., 1968) and it really is connected with it as it will be shown later on. Moreover, it explains the sense of the *limited transitivity of similarity* notion.

A complementary to the similarity measure is the *dissimilarity measure*.

Definition 2

If $\sigma(\omega',\omega'')$ is a similarity measure satisfying the Definition 1 then

$$\delta(\omega',\omega'') = 1 - \sigma(\omega',\omega'') \tag{6}$$

is called a *dissimilarity measure* described on the same Cartesian product Ω^2.

There are many possibilities to define a similarity measure satisfying the above-given definition as well as the corresponding dissimilarity measures. Three of them are presented below.

Similarity based on a distance measure. If Ω is a metric space where a distance measure r between pairs of its elements has been established then similarity measure can be defined as

$$\sigma(\omega',\omega'') = exp[-\beta \cdot r(\omega',\omega'')] \tag{7}$$

where β is a scaling parameter. It is clear that the conditions a/, b/ and c/ of Definition 1 are satisfied due to the distance measure properties. Moreover, condition d/ due to the triangular inequality of distance measure is also satisfied. Distance measure may here mean

an Euclidean, absolute, Chebyshevian, or any other of non-limited distance measures used in applications (Jain A.K., Murthy M.N., Flynn P.J., 1999).

Similarity based on angular distance. If Ω^+ is a positive sector of a linear vector space and $\angle(\omega',\omega'')$ denotes an angular measure between a pair of vectors in Ω^+ then a similarity measure can be defined as

$$\sigma(\omega',\omega'') = 1 - |sin[\angle(\omega',\omega'')]| \tag{8}$$

The reciprocity and symmetry of this similarity measure is evident. For proving the inequality (5 d) we shall denote $\alpha = \angle(\omega',\omega'')$, $\beta = \angle(\omega'',\omega''')$, $\gamma = \angle(\omega',\omega''')$ and remark that a) the angles between any vectors consisting of non-negative components cannot exceed $\pi/2$, b) for any ω', ω'', $\omega''' \in \Omega^+$ it is $|\alpha-\beta| \le \gamma \le \alpha+\beta$. Hence, assuming that $\alpha \ge \beta$ (this being a problem of denotation only) it follows from (7) that $\sigma(\alpha-\beta) \ge \sigma(\gamma) \ge \sigma(\alpha+\beta)$. However, from the convexity of $\sigma(\omega',\omega'')$ it also follows that

$\frac{\sigma(\beta)}{1} < \frac{\sigma(a+\beta)}{\sigma(a)}$ (see Fig. 6) what leads to the inequality $\sigma(\alpha)\cdot\sigma(\beta) < \sigma(\alpha+\beta) \le \sigma(\gamma)$ as it was to be shown •

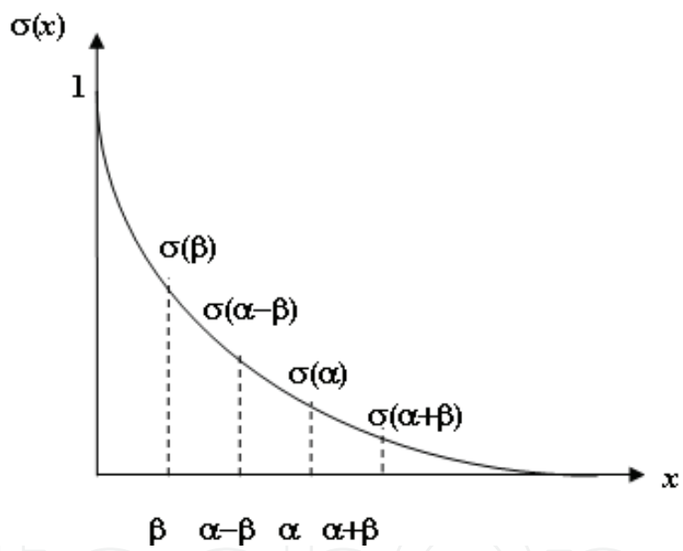

Fig. 6. Convexity of similarity measure based on angular distance.

Similarity based on logical tests. This type of similarity measure is particularly useful if some qualitative criteria to objects' similarity assessment are used. Such criteria may state, for example, that some external factors (noise, side anatomical details, lack of careful image preprocessing, etc.) could disturb the images and influence increasing the disparities. They also may state that difference of a qualitative feature characterizing the images is negligible. Let it will be defined a set of *N testing functions* (tests) of a general form

$$t_n: \Omega^2 \to \{0,1\}, \quad n = 1,2,\ldots,N, \tag{9}$$

assigning value 1 to a $t_n(\omega',\omega'')$ if (ω', ω'') satisfy a given condition confirming supposition of their similarity and value 0 otherwise. For the given series of tests $T = [t_1, t_2,\ldots, t_N]$, we denote by H the number of tests to which value 0 has been assigned. Then the similarity measure can be defined as

$$\sigma(\omega',\omega'') = \frac{N - H}{N + H} \tag{10}$$

Reciprocity and symmetry of the above-defined similarity measure is evident. The property (5d) follows, like before, from its convexity which for several values of N is shown in Fig. 7.
Similarity measures satisfying the conditions of Definition 1 have an important property making possible creation of multi-aspect similarity measures:

Theorem 1

Let $\sigma_1(\omega',\omega'')$, $\sigma_2(\omega',\omega'')$,…, $\sigma_k(\omega',\omega'')$ be similarity measures satisfying the conditions of Definition 1. Then

$$\sigma(\omega',\omega'') = \prod_{\kappa=1}^{k} \sigma_\kappa(\omega',\omega'') \tag{11}$$

is also a similarity measure in the sense of Definition 1.
Proof of this theorem is very simple, following directly from the Definition 1 •

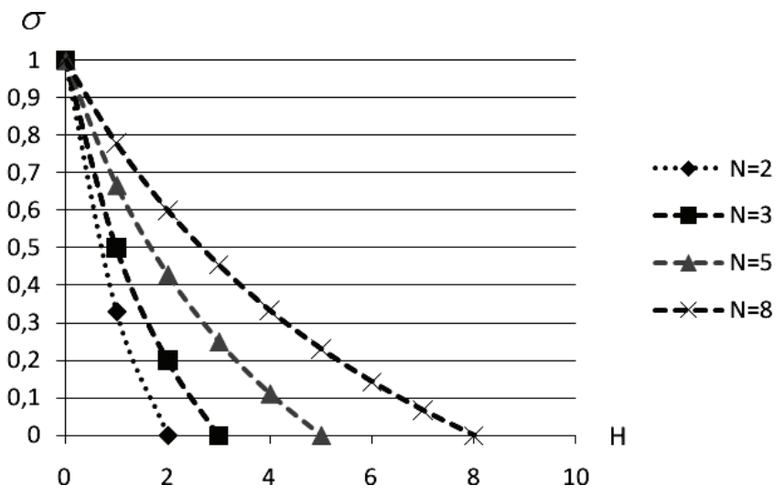

Fig. 7. Behavior of similarity measure based on logical tests.

It follows from this Theorem that if $\sigma(\omega',\omega'')$ is a similarity measure then $\sigma^\nu(\omega',\omega'')$ for any real $\nu > 1$ is a similarity measure as well. However, due to the inequality $\sigma^\nu(\omega',\omega'') \le \sigma(\omega',\omega'')$ such a similarity measure is more rigid than $\sigma(\omega',\omega'')$. Using $\sigma^\nu(\omega',\omega'')$ instead of $\sigma(\omega',\omega'')$ for $0 < \nu < 1$ leads to a reciprocal effect of similarity measure weakening. However, it cautiously can be used because for ν close to 0 convexity of $\sigma^\nu(\omega',\omega'')$ may be lost.
Using dissimilarity instead of similarity measure in comparative image analysis may be more convenient. Basic dissimilarity measure properties follow directly from the expression (6) and the corresponding similarity measure properties. In particular:

Theorem 3

If $\delta(\omega',\omega'')$ is a dissimilarity measure described on Ω^2 according to the Definition 2 then for any $\omega',\omega'', \omega''' \in \Omega^2$ the following inequality holds:

$$\delta(\omega',\omega''') \le \delta(\omega',\omega'') + \delta(\omega'',\omega''') - \delta(\omega',\omega'')\cdot\delta(\omega'',\omega'''). \tag{12}$$

Theorem 4

If $\delta_1(\omega',\omega'')$, $\delta_2(\omega',\omega'')$,… , $\delta_k(\omega',\omega'')$ are some dissimilarity measures described on Ω^2 then

$$\delta(\omega\ ',\omega\ '') = \prod_{\kappa=1}^{k} [1 - \delta_{\kappa}\ (\omega\ ', \omega\ '')] \tag{13}$$

is also a dissimilarity measure in the sense of Definition 2.
Proving validity of (12) and (13) consists in substitution of $1-\delta(\ )$ instead of $\sigma(\ )$, respectively, in (5 d) and (11) •

4. Description of textures by morphological spectra

4.1 Morphological spectra.

In Sec. 1 several possibilities of features selection for comparative image analysis have been mentioned. It also was remarked that environmental features better suit to a deep texture analysis than a point-to-point comparison of pixel values. The main difficulty in texture analysis lies in the randomness and multi-level morphological textures' structure. In most cases a texture is given as an instance of a random field whose statistical properties are not exactly known. Detection of textures dissimilarity is in fact a heuristic attempt to prove a hypothesis that the given two fragments of textures belong (or do not belong) to the same statistical population. For proving this hypothesis spatial relationships between pixel values visually observed as morphological texture features should be taken into consideration. One of possible ways to do it consists in using 2-dimensional spectral texture description. For this purpose, in principle, any complete system of bi-variable orthogonal functions can be used. However, any system of this type better or worse suits to morphological structures characterization and needs less or more sophisticated calculations. Morphological spectra seem to offer a compromise between calculation complexity and accuracy of textures description including their ability to describe them on several morphological organization levels.
We call morphological spectra a system of discrete bi-variable Walsh functions arranged in a hierarchical tree (Kulikowski J. L., Przytulska M. & Wierzbicka D. (2007a). For image description by morphological spectra selected *ROI*s are divided into square basic windows of $2^n \times 2^n$ size (see Fig. 2), n being a natural number called *spectrum level.* Each n-th level morphological spectrum is represented by 4^n spectral components. For the sake of presentation consistency, original image (U' or U'' defined by (1)) is considered as its 0-th level morphological spectrum. However, morphological spectrum of any fixed level contains full information about morphological spectra of any other level and into them can easily be transformed.
For calculation of morphological spectra special vectors called *spectral component masks* will be used.
Let us take into consideration the contents of μ-th basic window in a *ROI* represented by the vector $u_{\mu^*} = [u_{\mu 1}, u_{\mu 2}, \ldots, u_{\mu N}]$ (see (3)). Then, its four 1st level morphological spectrum components are given by the formulae:

$$\left.\begin{aligned} S &= [1,1,1,1] \cdot (u_{\mu^*})^{tr} = u_{\mu 1} + u_{\mu 2} + u_{\mu 3} + u_{\mu 4}, \\ V &= [-1,1,-1,1] \cdot (u_{\mu^*})^{tr} = -u_{\mu 1} + u_{\mu 2} - u_{\mu 3} + u_{\mu 4}, \\ H &= [-1,-1,1,1] \cdot (u_{\mu^*})^{tr} = -u_{\mu 1} - u_{\mu 2} + u_{\mu 3} + u_{\mu 4}, \\ X &= [-1,1,1,-1] \cdot (u_{\mu^*})^{tr} = -u_{\mu 1} + u_{\mu 2} + u_{\mu 3} - u_{\mu 4}, \end{aligned}\right\} \tag{14}$$

The same can graphically be presented as four *component masks* shown below:

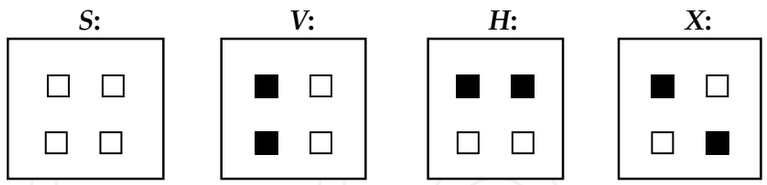

Fig. 8. Graphical masks of 1st level morphological spectrum components.

White marks denote the pixels in the basic window whose values should be taken with positive, while black – with negative sign in calculation of a sum corresponding to a given spectral component. A 1st level morphological spectrum of a given *ROI* consisting of *N* basic windows arranged into an $I \times J$ rectangular array ($I \times J = N$) will be given by four $I \times J$ real matrices collecting spectral components' values and denoted, respectively, by *S, V, H* and *X*. For calculation of the components of the next (i.e. 2nd) spectral level the matrices *S, V, H* and *X* are once more handled as original images: they are divided into 2×2 basic windows for which the spectral components *S*, V, *H* and *X* are calculated. Therefore, from the spectral matrix *S* next, 2nd level spectral matrices denoted by *SS, VS, HS* and *XS* are obtained, their seize being reduced to $\frac{1}{2}I \times \frac{1}{2}J$. Similarly, the spectral matrices *V, H* and *X* respectively generate the 2nd level spectral matrices *SV, VV, HV, XV, SH, VH, HH, XH, SX, VX, HX* and *XX*. This, iterative procedure can be used for higher-level spectral components. The components of morphological spectra can thus be presented in the form of a hierarchical tree shown in Fig. 9.

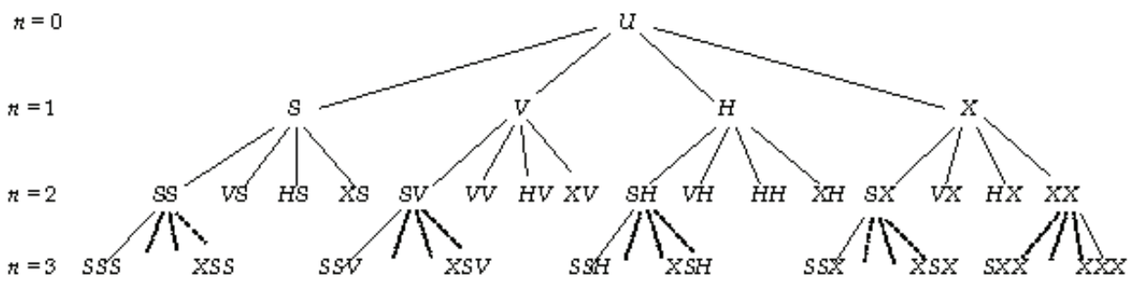

Fig. 9. Hierarchical tree of morphological spectral components.

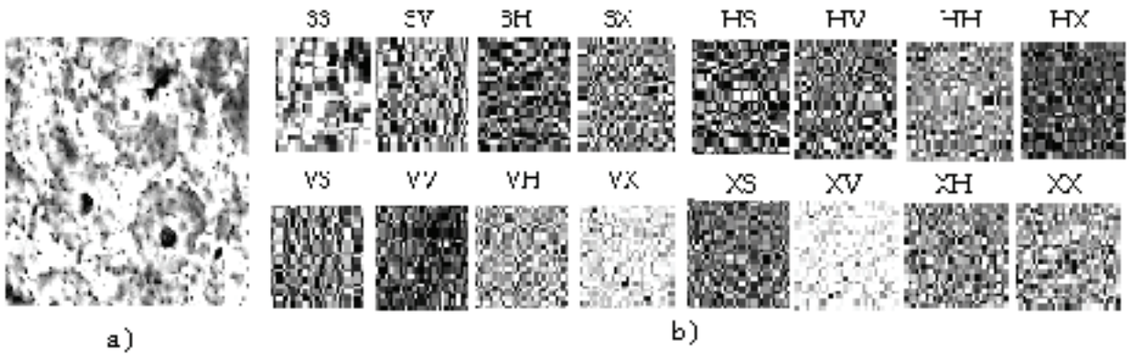

Fig. 10. Original image a) and its morphological spectral components b) of a bone section.

In Fig. 10 a 128×128 pixels-size *ROI* presenting texture of a bone section and 16 its 2nd level morphological spectral components are shown. It can be noticed that intensities of different components are different due to the fact that different micro-morphological details are by them represented.

4.2 Statistical analysis of morphological spectra.

Symbolic denotations of spectral components can also be interpreted as linear transformations which should be performed (from the right to left) on the image in order to get the corresponding component value. Transformation S (see (14)) plays a role of details smoothing operation: standing on the right side of the component's name it averages pixel values and reduces the image resolution power, while standing on the left side it averages on larger areas the former transformations results as it can be observed in Fig. 11.

Like the original image of a texture, its spectral components can be considered as instances of some random fields. Their direct interpretation is rather difficult; however, for comparative lesions detection they can be subjected to a statistical data processing. It should be remarked that spectral components of a given image are in general not statistically independent. Their cross-correlations thus can be used to a reduction of data necessary to aneffective lesions detection (Kulikowski J. L., Przytulska M. (2009b). However, for the sake of simplicity of lesions detection procedures statistical dependence of spectral components can in practice be neglected. Moreover, in order to avoid an effect of parallel image shift sensitivity of the results of spectral texture analysis using absolute spectral components instead of their original, real magnitudes is reasonable. For basic parameters characterizing statistical properties of the spectral components calculation, first, *histograms* (experimental probability densities) of their intensity in the given *ROI* should be calculated. For this purpose, instead of single matrices U', U'' (see (1)-(4)) used to contents of selected *ROI*s presentation sets of spectral matrices can be used. Let us denote by $\Lambda^{(n)}$ the set of symbolic names of n-th level spectral components and let λ be a shortly denoted symbolic name of a spectral component. We denote by $v_{\mu^*} = [v_{\mu\lambda}]$, $\lambda \in \Lambda^{(n)}$, a vector of spectral components of μ-th basic window of the considered *ROI*, $\mu \in [1,2,\ldots,M^{(n)}]$, ($M^{(n)}$ being 4^n times reduced with respect to the number M of pixels in the original *ROI*). Then, the spectral *ROI* representation will be given by a matrix $V^{(n)}$ composed of $M^{(n)}$ rows v_{μ^*} describing the spectra of basic windows. A λ-th column $v_{*\lambda}$ of $V^{(n)}$ consists of the λ -component values in the basic windows of the *ROI*. Any statistical parameters of spectral components should be thus calculated on the corresponding $V^{(n)}$ columns considered as random vector's instances. For a $v_{*\lambda}$ component's histogram $h_\lambda(\delta)$ calculation the minimal $v_{\lambda\,min}$ and maximal $v_{\lambda\,max}$ values in the column $v_{*\lambda}$ first should be found.

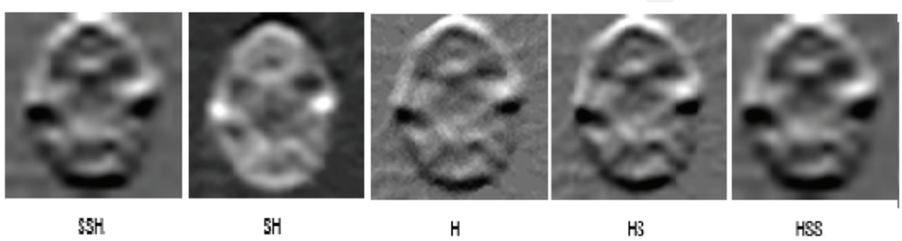

Fig. 11. Effects of image details smoothing by the S operation used after (*SH, SSH*) and before (*HS, HSS*) the basic operation H performed on a *SPECT* image of a brain.

Then, according to the desired statistical parameters estimation accuracy, an interval length

$$\beta = \frac{v\lambda \max - v\lambda \min}{\Delta - 1} \tag{15}$$

where $\Delta > 1$ is a fixed natural number, should be calculated. On the abscissa axis Δ left-open right-closed intervals:

$$b_\delta = (v_{\lambda\, min} + (\delta - 1 - ½)\beta,\ v_{\lambda\, min} + (\delta - 1 + ½)\beta], \quad \delta \in [1,2,\ldots,\Delta] \tag{16}$$

of δ length should be chosen and for each b_δ the number n_δ of the elements of $v_{*\lambda}$ whose values fall into b_δ should be evaluated. The histogram is then defined as a vector $h_\lambda(\delta) = [h_1, h_2,\ldots,h_\Delta]$ whose components are given by the frequency rates:

$$h_\delta = \frac{n_\delta}{M^{(n)}} \tag{17}$$

Of course, it should be $\sum_{\delta=1}^{\Delta} n\delta = M^{(n)}$. In Fig. 12 several histograms of morphological spectra components are shown. For comparison, the 1st level, S and X components of ultrasound liver imaging in a normal and liver fibrosis diagnosed patients have been chosen. The visual differences between the diagrams seem rather small. However, the beside shown estimated parameters of the histograms exhibit non-negligible differences: the histograms in ill patients are shifted to the right. This becomes evident if the minimal and mean values of the corresponding spectral components in normal and ill patients are compared. This example illustrates the idea of using morphological spectra as source of parameters suitable to comparative lesions detection. For this purpose, the following widely used parameters can be calculated and used:

- *Minimal, $v_{\lambda\, min}$ and maximal, $v_{\lambda\, max}$ component values*;
- *Statistical mean*:

$$m\lambda = \sum_{\delta=1}^{\Delta} \delta\, h\delta \tag{18}$$

- *Median*:

$$med_\lambda = \delta^* \text{ such that } \sum_{\delta=1}^{\delta^*-1} n\delta < \frac{M^{(n)}}{2} \le \sum_{\delta=1}^{\delta^*} n\delta \tag{19}$$

- *Standard deviation*:

$$sdev\lambda = \sqrt{\frac{1}{(M^{(n)}-1)} \sum_{\delta=1}^{\Delta} (\delta - m\lambda)^2\, n\delta} \tag{20}$$

- *Skewness*:

$$sk\lambda = \frac{1}{\Delta} \frac{\sum_{\delta=1}^{\Delta} (\delta - m\lambda)^3}{(sdev\lambda)^3} \tag{21}$$

- *Kurtosis*:

$$kurt\lambda = \frac{\Delta}{(\Delta - 2)(\Delta} \sum_{\delta=1}^{\Delta} \frac{(\delta - m\lambda)^4}{(sdev\lambda)^4} - \frac{3(\Delta - 1)^2}{(\Delta - 2)(\Delta - 3)} \tag{22}$$

- *Entropy*:

$$H\lambda = - \sum_{\delta=1}^{\Delta} h\delta \ln(h\delta) \tag{23}$$

etc.

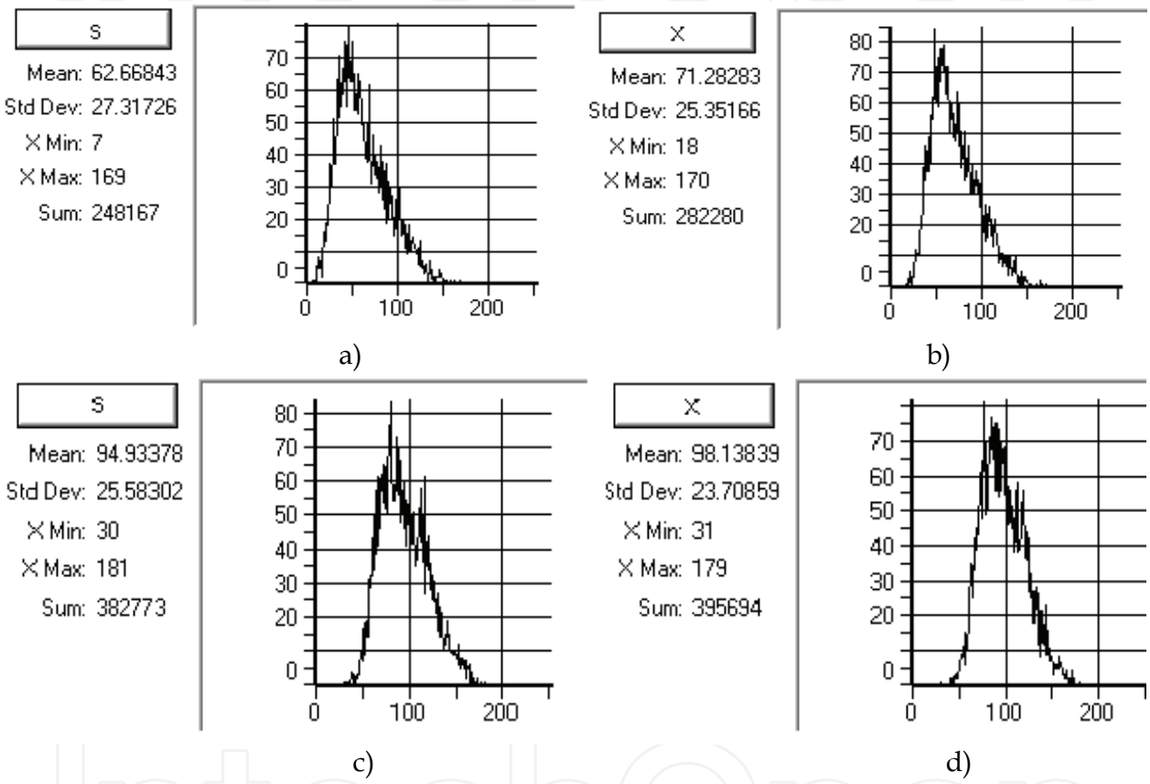

Fig. 12. Histograms of selected liver tissue morphological spectra components:
a) *S* component in a normal patient, b) *X* component in the normal patient,
c) *S* component in an ill (liver fibrosis diagnosed) patient, d) *X* components in the ill patient.

Finally, for each λ-th spectral component we get a sequence of F estimated parameters $w_{*\lambda} = [w_{1\lambda}, w_{2\lambda}, \ldots, w_{F\lambda}]^{tr}$ (for the sake of convenience presented here in transposed, horizontal form). For further considerations, the contents of compared *ROI*s instead of their original images U', U'' will thus be presented by two matrices W', W'' of $F \times L$ size, L denoting the number of spectral components selected for image analysis ($L \leq 4^n$), composed of the corresponding column-vectors $w'_{*\lambda}$, $w''_{*\lambda}$.

4.3 Statistical aspects of textures' similarity.

On the basis of morphological spectra the notion of textures' similarity can be formulated so that the randomness of textures is taken into consideration.

Definition 3
A set of objects $\Xi = \{u_{\mu^*}\}$ described by their morphological spectra v'_{μ^*} is called a *fuzzy* e*-similarity class* if for a given real non-negative vector $e = [e_\lambda]$, $\lambda \in \Lambda^{(n)}$, standard deviations $sdev_\lambda$ of its spectral components satisfy the inequalities

$$sdev_\lambda \leq e_\lambda . \tag{24}$$

Taking into account that various spectral components in textures similarity establishment may be of different importance, the inequalities (24) can be used as basis of a multi-aspect similarity measure based on logical tests. For different spectral components or their algebraic combinations different tests and final similarity criterion, according to Theorem 1, as their product can be established. In similar way, a dissimilarity of a pair Ξ', Ξ'' of objects can be defined.

Definition 4
For a given dissimilarity measure δ and a fixed d, $0 \leq d \leq 1$, two texture instances u'_{μ^*}, u''_{μ^*} are called *fuzzy d-dissimilar* if their morphological spectra v'_{μ^*}, v''_{μ^*} satisfy the condition

$$\delta(v'_{\mu^*}, v''_{\mu^*}) \geq d. \tag{25}$$

In this case, the dissimilarity measure can also be defined as multi-aspect, constructed according the Theorems 3 and 4, based on all estimated statistical parameters of morphological spectra.

5. General remarks on multi-aspect comparative detection of lesions

To the above-defined notions of fuzzy e-similarity and fuzzy d-dissimilarity in application to lesions detection a medical interpretation can also be assigned. A notion of medical diagnostic test's *sensitivity* is related to its ability to detect with high accuracy existence of a pathological factor. In comparative lesions detection this property is connected with ability to assign high dissimilarity measure to the textures of a normal and a pathological tissue. On the other hand, a diagnostic test's *specificity* means its ability to neglect seemingly pathological factors. In comparative lesions detection this means that high similarity measure is assigned to the basic windows within the same (normal or pathological) *ROI*. It might seem that both, high sensitivity and high specificity of lesions detection can easily be reached by choosing the (in Definitions 3 and 4 mentioned) threshold levels e and d as low as possible. However, it is not so. Low d means high that highly similar textures could be decided different. Moreover, it might happen in this case that certain objects are decided both, e-similar and d-dissimilar to a given set Ξ. In order to avoid this situation d should be chosen so that an intersection of the fuzzy e-similarity and (1– d)-similarity classes is reduced. However, this situation may on the other hand lead to existence of objects e-similar neither to Ξ' nor to Ξ''. The effect of strengthening the dissimilarity criterion by threshold d is illustrated in Fig. 13. For a 128×128 size *SPECT* image of brain (compare Fig. 2) absolute value of spectral component *SX*, as most sensible to fine local texture granularity, was calculated. Then, a difference of this component between the right and left cerebral hemisphere was taken into consideration as a parameter characterizing the disparities between the corresponding 4×4 basic windows in the two *ROI*s covering the hemispheres. The spectral images b), c) and d) are presented in artificially increased scale, compensating the effect of their size reduction caused by basic windows increasing. Logical dissimilarity

test consisted in checking the difference value exceeding a threshold level d_{SX} . Higher threshold level brings to a reduction of detected local disparities.

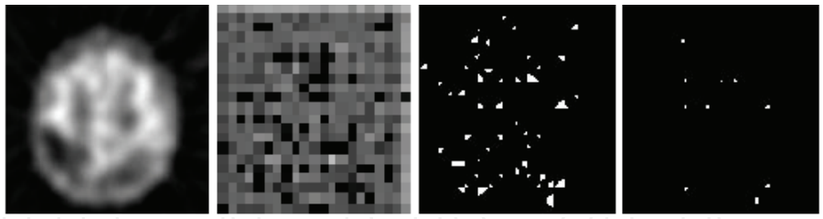

a) b) c) d)

Fig. 13. Disparities detection in cerebral *SPECT* image: a) original image, b) its morphological *X* component, c) disparities on low dissimilarity level, d) disparities on high dissimilarity level.

Hence, it follows from the analysis and example that **reaching simultaneously a detection rule of high sensitivity and high specificity is impossible**. Taking this basic constraint into account one can formulate the comparative lesions detection problem as follows:

Assume that Ξ' and Ξ'' are two subsets of objects in X^N considered as instances of two statistical populations. Let there be given criteria of fuzzy similarity of objects within the separately taken populations and fuzzy dissimilarity of objects belonging to different populations, based on estimated statistical parameters of the populations. Check: a) the fuzzy similarity requirement being satisfied by Ξ' and Ξ'', b) in positive case – the requirement of fuzzy dissimilarity of Ξ' and Ξ''.

This problem formulation does not settle the necessity of using morphological spectra to textures description. The concepts of multi-aspect similarity measure and dissimilarity measure admits using combinations of various types of objects description. However, statistical nature of textures forces preferring fuzzy similarity and dissimilarity concepts with respect to their deterministic versions. It also should be remarked that if fuzzy similarity of Ξ' and Ξ'' is not satisfied, checking their dissimilarity is pointless; such situation may arise if *ROI*s have been delineated on the borders between different textures.

Statistical nature of textures leads also to another type of limitation. Fuzzy similarity and dissimilarity of sets of instances of random objects can be the more accurately established the larger are the populations. This leads to a necessity of *ROI*s containing large number of basic windows delineation. However, this means that small-area lesions are poorly detectable. Therefore, **the requirements of high lesions detection sensitivity and of high accuracy of small lesions localization can not be together satisfied**. This can be considered as a sort of *uncertainty principle* in lesions detection.

A general scheme of comparative lesions detection realizing the above-presented concept based on morphological spectra application is shown in Fig. 14. In reaching high effectiveness of lesions detection selection of spectral components, choosing their statistical parameters and construction of similarity and dissimilarity measures play a crucial role. This can be reached by experiments rather than by solving a typical mathematical optimization problem. Moreover, experiments performed on different types of textures usually lead to different recommendations for choosing satisfactory solutions. In particular, it is necessary to distinguish isotropic and anisotropic biological tissues and to chose adequate to this combinations of spectral components for texture analysis. The *S*- and *X*-type operations are insensible to the anisotropy of texture, *V*-type operation is sensible to

vertical, while *H*-type to horizontal structures. Therefore, in anisotropic textures analysis combinations of spectral components containing *V*- and *H*-operators (e.g. *SH* and *SV*, *XVH* and *XHV*, etc.) equally should used.

7. Conclusion

Comparative lesions detection is a well known technique used in medical diagnosis. It is based on an assumption that even if not only the existence, but also the form, size, location in patient's body, etc. of a lesion are not a priori known, nevertheless, it can be assumed that they exhibit differences with respect to a normal body. To detection of such differences

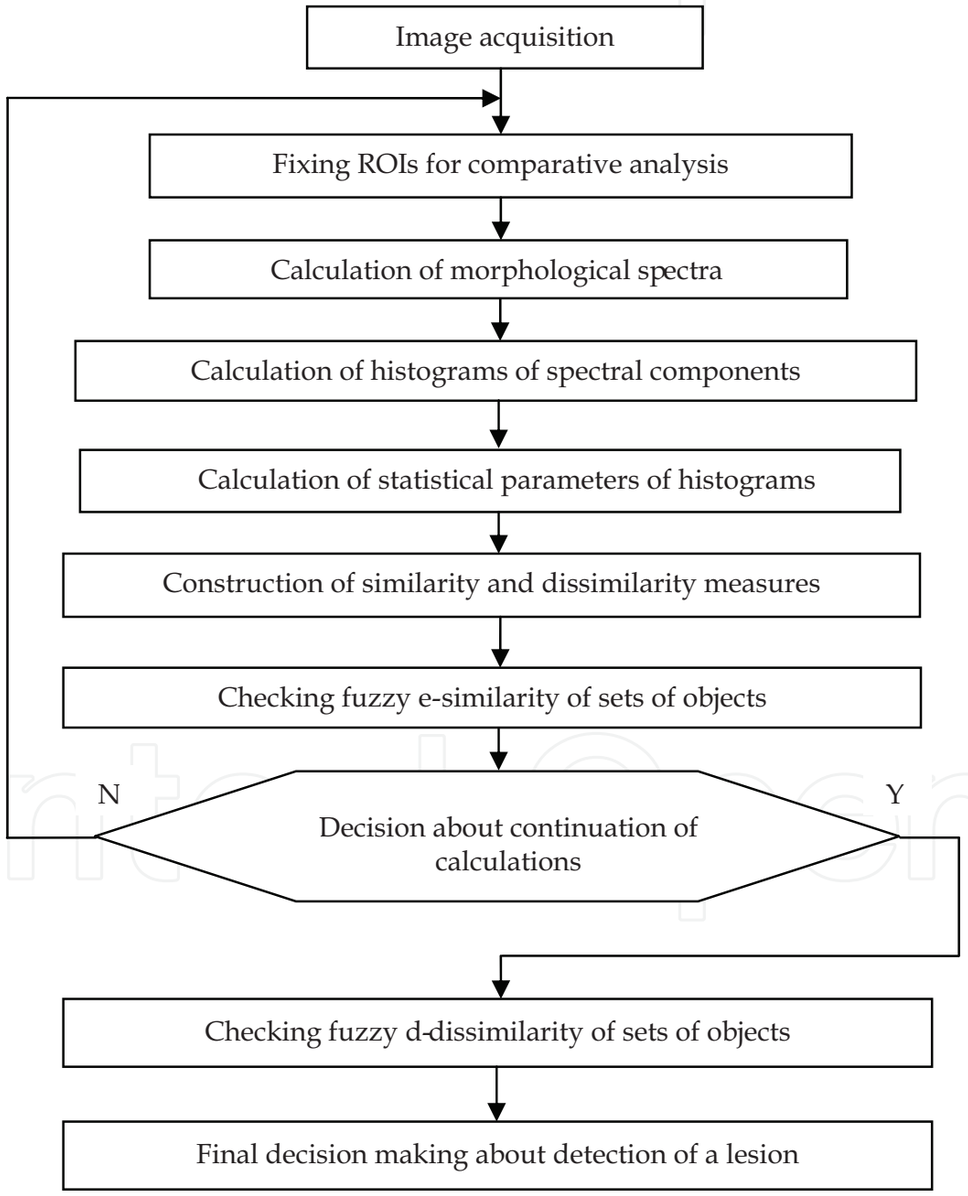

Fig. 14. Scheme of comparative lesions detection algorithm based on morphological spectra.

various approaches can be used. All they should satisfy the requirement of high sensitivity and specificity of lesions detection. Unfortunately, the requirements are in a sort of contradiction leading to the necessity of choosing a compromise between them. Moreover, a simultaneous reaching high detection effectiveness and high accuracy of lesion's localization in the body is also limited. The above-mentioned difficulties inspire looking for advanced lesions detection methods based on new concepts and effective mathematical tools.

The above-presented concept of multi-aspect similarity measures based on strongly defined assumptions, in combination with this of morphological spectra and on some standard statistical methods seems generally to satisfy those expectations. Nevertheless, at a present state it still needs more experiments to be verified on large and more diversified sets of clinical data.

8. References

Bonner R.E., (1954). On some clustering techniques. *IBM Journal Research and Development*, No 8, 22-32.

Foley J.D., Van Dan A., Feiner S.K. & al. (1994). *Introduction to Computer Graphics.* Addison-Wesley Publishing Comp. Inc., ISBN 83-204-1840-2, Reading Massachusetts.

Gotlieb C.C., Kumar S., (1968). Semantic clustering of index terms. *Journal of the ACM,* Vol.15, No 4, 493-513.

Hornby A.S. (1980). *Oxford Advanced Learner's Dictionary of Current English.* University Press, ISBN 83-01-02448-8, Oxford.

Jain A.K., Murthy M.N., Flynn P.J. (1999). Data clustering: a review. *ACM Computing Surveys*, Vol. 31, No 3, 264-323.

Kulikowski J. L. (2001). Pattern Recognition Based on Ambiguous Indications of Experts. In: *Computer Recognition Systems, KOSYR'2001*. Kurzynski M. & al. (Ed.), 15-22,.OW Politechniki Wrocławskiej, Wrocław.

Kulikowski J.L., Przytulska M. & Wierzbicka D. (2007a). Recognition of Textures Based on Analysis of Multilevel Morphological Spectra. *GESTS International Transactions on Computer Science and Engineering* Vol. 38, No 1, March, 99-107, ISSN 1738-6438.

Kulikowski J.L., Przytulska M, & Wierzbicka D., (2007b). Morphological Spectra as Tools for Texture Analysis. In: *Computer Recognition Systems 2,* Kurzyński M. & al. (Ed.), 510-517, Springer-Verlag, ISBN-13*978-3-540-75174-8, Berlin Heidelberg New York.

Kulikowski J.L., Przytulska M. & Kuraszkiewicz B. (2009a). Segmentation of Radiological Images Based on Dissimilarity Measure, In: *Image Processing & Communications Challenges,* Choras R.S., Zabludowski A. (Ed.), 326-333, APH EXIT, Warsaw.

Kulikowski J.L., Przytulska M. (2009b). Biomedical Image Segmentation Based on Aggregated Morphological Spectra. In: *Computers in Medical Activity*. Kacki E. (Ed.), 101-112, Springer, Berlin.

Rasiowa H., Sikorski R. (1968). *The mathematics of metamathematics.* PWN – Polish Scientific Publishers, Warsaw.

Rogowska J., Preston K., Hunter G.J. & al., (1995). Application of similarity mapping in dynamic MRI. *IEEE Tran. Med. Imaging,* vol. 14, 480-486.

Lester H., Arrige S.R., (1999). A survey of hierarchical non-linear medical image registration. *Pattern Recognition*, vol. 32, 129-149.

Biomedical Engineering, Trends, Research and Technologies

Edited by Dr. Sylwia Olsztynska

ISBN 978-953-307-514-3
Hard cover, 644 pages
Publisher InTech
Published online 08, January, 2011
Published in print edition January, 2011

This book is addressed to scientists and professionals working in the wide area of biomedical engineering, from biochemistry and pharmacy to medicine and clinical engineering. The panorama of problems presented in this volume may be of special interest for young scientists, looking for innovative technologies and new trends in biomedical engineering.

InTech Europe
University Campus STeP Ri
Slavka Krautzeka 83/A
51000 Rijeka, Croatia
Phone: +385 (51) 770 447
Fax: +385 (51) 686 166
www.intechopen.com

InTech China
Unit 405, Office Block, Hotel Equatorial Shanghai
No.65, Yan An Road (West), Shanghai, 200040, China
中国上海市延安西路65号上海国际贵都大饭店办公楼405单元
Phone: +86-21-62489820
Fax: +86-21-62489821

IntechOpen